Spatial and interannual variability of dissolved organic matter in the Kolyma River, East Siberia, observed using satellite imagery

Claire G. Griffin,[1,2] Karen E. Frey,[1] John Rogan,[1] and Robert M. Holmes[3]

Received 20 December 2010; revised 13 May 2011; accepted 1 June 2011; published 10 August 2011.

[1] The Kolyma River basin in northeastern Siberia, the sixth largest river basin draining to the Arctic Ocean, contains vast reserves of carbon in Pleistocene-aged permafrost soils. Permafrost degradation, as a result of climate change, may cause shifts in riverine biogeochemistry as this old source of organic matter is exposed. Satellite remote sensing offers an opportunity to complement and extrapolate field sampling of dissolved organic matter in this expansive and remote region. We develop empirically based algorithms that estimate chromophoric dissolved organic matter (CDOM) and dissolved organic carbon (DOC) in the Kolyma River and its major tributaries in the vicinity of Cherskiy, Russia. Field samples from July 2008 and 2009 were regressed against spectral data from the Landsat 5 Thematic Mapper and Landsat 7 Enhanced Thematic Mapper-Plus. A combination of Landsat band 3 and bands 2:1 resulted in an R^2 of 0.78 between measured CDOM and satellite-derived predictions. Owing to the strong correlation between CDOM and DOC, the resulting maps of the region show strong interannual variability of both CDOM and DOC, and important spatial patterns such as mixing zones at river confluences and downstream loading of DOC. Such variability was previously unobserved through field-based point observations and suggests that current calculations of DOC flux from the Kolyma River to the Arctic Ocean may be underestimates. In this era of rapid climate change, permafrost degradation, and shifts in river discharge, remote sensing of CDOM and DOC offers a powerful, reliable tool to enhance our understanding of carbon cycling in major arctic river systems.

Citation: Griffin, C. G., K. E. Frey, J. Rogan, and R. M. Holmes (2011), Spatial and interannual variability of dissolved organic matter in the Kolyma River, East Siberia, observed using satellite imagery, *J. Geophys. Res.*, *116*, G03018, doi:10.1029/2010JG001634.

1. Introduction

[2] Impacts of climate change are already well-observed in high-latitude regions, including increased river discharge, lake disappearance, permafrost degradation, coastal erosion, sea ice reduction, and glacier and ice sheet melt [*Peterson et al.*, 2002; *Arctic Climate Impact Assessment* (*ACIA*), 2005; *Smith et al.*, 2005; *McClelland et al.*, 2006; *Frey et al.*, 2007; *Wang and Overland*, 2009]. Biogeochemical cycling in arctic watersheds is undoubtedly heavily influenced by changes in permafrost, hydrology and ecosystem dynamics, as a result of regional climate warming [*ACIA*, 2005]. For instance, northern high-latitude permafrost regions hold ~1672 Pg of carbon, accounting for ~50% of the global belowground organic pool [*Tarnocai et al.*, 2009]. Permafrost degradation will likely lead to the release of significant portions of this old and potentially labile carbon, contributing an important positive feedback to climate warming [*Frey and McClelland*, 2009].

[3] Dissolved organic matter (DOM) in permafrost-dominated arctic rivers has two main sources: (1) detrital material that has accumulated on the land surface from the previous growing season and subsequently leached into rivers [*Spencer et al.*, 2008, 2009]; and/or (2) DOM that has leached from the soil column or active layer in permafrost environments into adjacent streams and rivers during warmer summer months [*Moore*, 2003; *Raymond et al.*, 2007]. Either of these sources could be altered as a result of climate change [*Wickland et al.*, 2007], with subsequent changes in DOM inputs to arctic rivers that may have impacts on both in-stream processing [*Cole et al.*, 2007; *Battin et al.*, 2009] and coastal productivity [*Cooper et al.*, 2005; *Frey et al.*, 2007; *Anderson et al.*, 2009]. The Arctic Ocean is heavily influenced by river inputs as it consists of only ~1% of the world's ocean volume, but receives ~10% of global river discharge and riverine DOM [*Opsahl et al.*, 1999; *Dittmar and Kattner*, 2003; *Holmes et al.*, 2011]. Potential increases in riverine DOM flux may alter carbon cycling in coastal arctic environments, through both bacte-

[1]Graduate School of Geography, Clark University, Worcester, Massachusetts, USA.
[2]Now at Marine Science Institute, University of Texas at Austin, Port Aransas, Texas, USA.
[3]Woods Hole Research Center, Falmouth, Massachusetts, USA.

0148-0227/11/2010JG001634

rial respiration and/or nutrient remineralization leading to increased primary production [*Garneau et al.*, 2008; *Holmes et al.*, 2008]. The fate of DOM in high-latitude inland waters and coastal environments thus needs to be better quantified to understand the potential impacts of climate change on arctic carbon cycling [*Cole et al.*, 2007; *Battin et al.*, 2009]

[4] Recent studies and monitoring programs have highlighted the extreme spatial and seasonal heterogeneity across the pan-Arctic region. Projections of DOM export, based on field observations, differ between watersheds, likely owing to differences in organic carbon content in near-surface soils that may thaw in a warming climate [*Frey and McClelland*, 2009]. Modeling efforts predict that permafrost-free regions in the West Siberian Lowland could double in area by the end of the century, leading to a 29–46% increase in dissolved organic carbon (DOC) export by 2100 from this region [*Frey and Smith*, 2005]. A number of high-latitude rivers in Europe and North America have also experienced increased DOC concentrations in recent decades [*White et al.*, 2007, and references therein]. However, observations in the Yukon River show a decrease in discharge-normalized DOC export between the late 1970s and early 2000s [*Striegl et al.*, 2005]. Such decreases in DOC are likely due to increased hydrologic flow paths, residence times, and microbial mineralization of DOC in the active layer or in groundwater pathways [*Striegl et al.*, 2005].

[5] In addition to these differences between river basins, arctic rivers also experience extreme seasonal variability in their biogeochemical characteristics. High-latitude rivers are highly seasonal, characterized by low discharge during the winter months followed by a peak flow during spring snowmelt and a more gradual decrease in discharge throughout the summer [*Raymond et al.*, 2007]. DOC concentrations generally increase with discharge in these rivers, resulting in the majority of carbon flux to the Arctic Ocean occurring during spring snowmelt (May–June) [*Raymond et al.*, 2007; *Holmes et al.*, 2008, 2011]. This early season DOC is young (typically less than 20 years old) and originates largely from terrestrial plant matter from recent growing seasons [*Finlay et al.*, 2006; *Neff et al.*, 2006; *Raymond et al.*, 2007; *Stedmon et al.*, 2011]. In contrast, *Neff et al.* [2006] demonstrated that in the Kolyma River basin, late season DOC was largely composed of old carbon that had previously been stable for thousands of years. Early season DOC flux may change owing to ongoing shifts in vegetation, productivity, and precipitation, but monitoring summer DOC (July–October) may be critical to assessing whether permafrost degradation is leading to the release of old and potentially labile carbon [*Finlay et al.*, 2006; *Neff et al.*, 2006]. These dramatic variations in DOM export only highlight the need for continued monitoring of river biogeochemistry from a variety of watersheds across the pan-Arctic region.

[6] The majority of measurements of DOM or DOC in arctic rivers are point samples on large river main stems within a relatively limited time frame. Until recently, most field campaigns have focused almost solely upon summer sampling, and many still consist of only a few samples dispersed throughout the ice-free season [e.g., *McClelland et al.*, 2008; *Stedmon et al.*, 2011]. Satellite remote sensing can provide a consistent method to supplement and extrapolate direct sampling and fill gaps between field campaigns. While satellite imagery cannot directly measure the amount of DOC in water bodies, it can be used to estimate concentrations of the colored fraction of DOM, or chromophoric dissolved organic matter (CDOM) [*Coble*, 2007]. CDOM is highly correlated with DOC in arctic rivers and streams [*Spencer et al.*, 2009; *Stedmon et al.*, 2011], allowing for remote sensing to indirectly measure DOC from satellite imagery. Indeed, remote sensing is regularly used in coastal and lake studies to map CDOM [*Twardowski et al.*, 2005; *Olmanson et al.*, 2008]. The spectral properties of a water body are influenced by CDOM, chlorophyll, particulates and detritus, and the water itself, such that field sampling is necessary to create region-specific empirically based algorithms to estimate CDOM [*Coble*, 2007]. Moderate Resolution Imaging Spectroradiometer (MODIS) and Sea-viewing Wide Field-of-view Sensors (SeaWiFS) have been used successfully to map CDOM or DOC in coastal arctic waters [e.g., *Retamal et al.*, 2007], but do not have appropriate spatial resolution for use in most inland waters. While high spatial resolution hyperspectral data, such as the Advanced Land Imager, may be ideal for estimating CDOM [*Kutser et al.*, 2005a, 2005b], Landsat Thematic Mapper (TM) and Enhanced Thematic Mapper Plus (ETM+) data have successfully been used to model water properties of subarctic and temperate lakes [*Brezonik et al.*, 2005; *Kallio et al.*, 2008]. The Landsat platform has the advantages of high spatial resolution (30 m), high temporal resolution (16 d), and a data record that extends back to the 1970s [*Rogan and Chen*, 2004]. Furthermore, Landsat band ratios (e.g., red to green or red to blue) and multiple linear regression has led to the development of empirical algorithms relating spectral characteristics and CDOM with R^2 values ≥ 0.70 [e.g., *Brezonik et al.*, 2005].

[7] The Kolyma River in northeastern Siberia (Figure 1) exemplifies an Arctic region for which field observations are typically sporadic. As with other large arctic rivers, the Kolyma is characterized by a "flashy" hydrograph in the spring, followed by stable summer base flow July through September (Figure 2), with a mean annual discharge of 132 km^3. The Kolyma basin is approximately 650,000 km^2 in area and is the largest Arctic river basin completely underlain by continuous permafrost [*Holmes et al.*, 2011]. These permafrost-influenced soils, called yedoma, are characterized by 10–90 m thick Pleistocene-aged, icy loess deposits, containing 3–5% organic carbon [*Zimov et al.*, 2006a]. Long-term monitoring of Kolyma River biogeochemistry began in late 2003, with samples collected multiple times per year during the ice-free season at Cherskiy, Russia [*McClelland et al.*, 2008; *Holmes et al.*, 2011]. In addition, expansive sampling conducted in July 2008 and July 2009 revealed large spatial variability between the Kolyma River and its tributaries [*Holmes et al.*, 2009], in addition to the seasonal and interannual variability previously observed [*Holmes et al.*, 2011]. Mapping CDOM in the Kolyma using remote sensing allows for temporal and spatial extrapolation of these river biogeochemistry field observations to also include years without field campaigns and provide estimates of CDOM for major river tributaries previously unavailable.

[8] The goal of this study was to quantify the spatial and interannual variability in DOM within the Kolyma River to enhance the understanding of organic matter fluxes to the Arctic Ocean, particularly in summer months when most

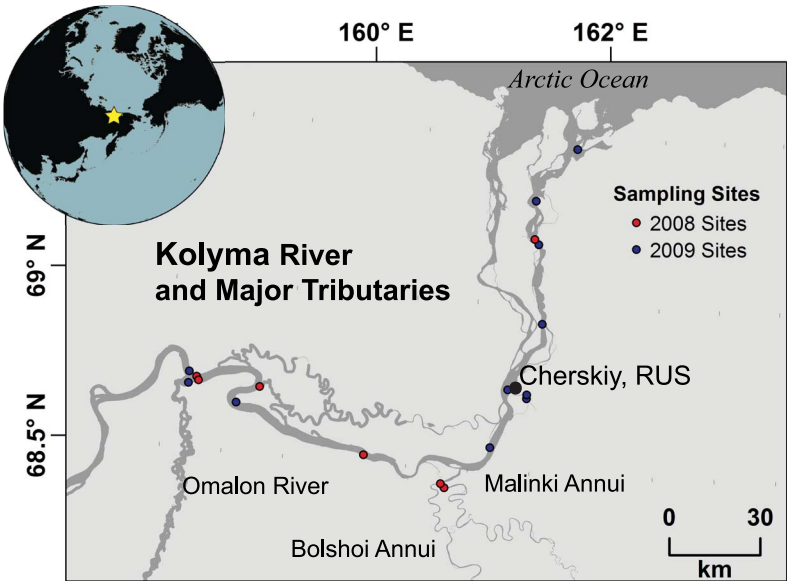

Figure 1. Study area of the lower Kolyma River. Field campaigns were based out of Cherskiy, Russia, with samples extending approximately 250 km along the Kolyma River main stem. The sampling sites from July 2008 and 2009 used to create an empirical model estimating chromophoric dissolved organic matter (CDOM) from Landsat satellite are also shown.

organic matter is derived from old permafrost soils. Specifically, satellite data from the past decade were used to map CDOM values throughout the lower Kolyma, thus expanding the record of DOM to include years that were not sampled in situ, and add previously unobserved information about spatial patterns of DOM distribution. To achieve these goals, we present spatially extensive field-based measurements of CDOM and DOC collected July 2008 and 2009. Linear regression models were developed to relate these field-based measurements to Landsat data, then applied to spectrally enhanced Landsat data collected during summer over the last decade (2000–2010) to observe broad spatial patterns and interannual variability in DOC and CDOM concentrations. The results of this study suggest that previous estimates of DOM fluxes (that do not incorporate our new observations of high spatial variability in concentrations) may underestimate the true export of DOM.

2. Data and Methods

2.1. Field Sampling

[9] Field sampling campaigns were based out of the Northeast Science Station near Cherskiy (68°47′N, 161°20′E), Russia, in northeastern Siberia (Figure 1), as part of the

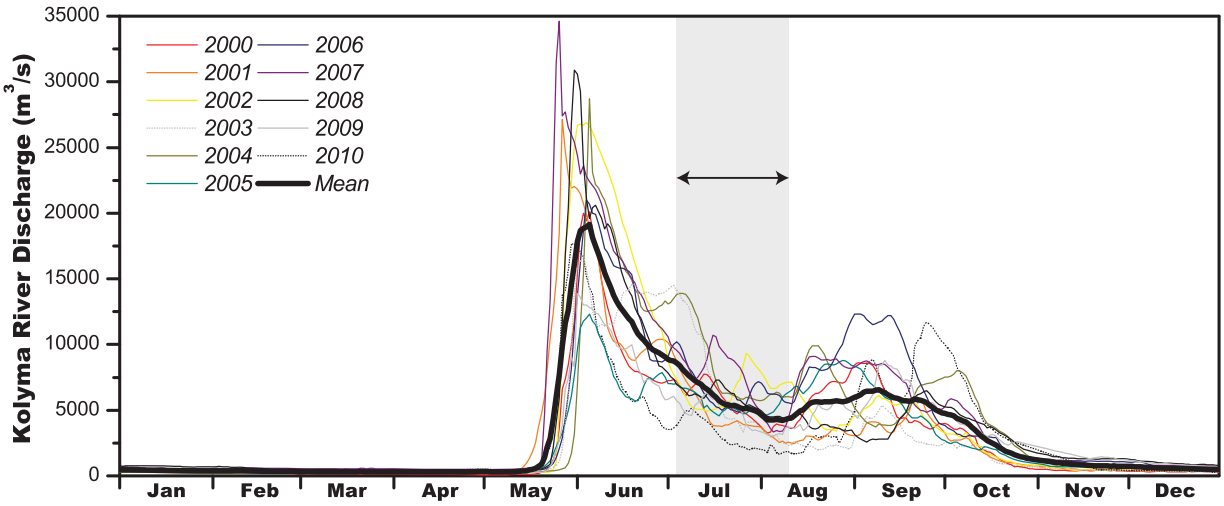

Figure 2. Daily discharge of the Kolyma River (adjusted to Cherskiy, Russia, 160 km downstream of the gauging station) for the years 2000–2010 (color coded lines) and mean discharge (black line). The Kolyma is characterized by peak flow in early June, followed by summer base flow. There is often a less pronounced peak in discharge late in the summer, usually during late August or September. The grayed out area of the hydrographs indicates the timeframe examined in this study (6 July through 10 August).

Table 1. Landsat TM and ETM+ Imagery Used in This Study[a]

Satellite	Acquisition Date	Path/Row	Use
Landsat 7 ETM+	24 Jul 2010	106/11	Mapping CDOM
Landsat 7 ETM+	24 Jul 2010	106/12	Mapping CDOM
Landsat 5 TM	31 Jul 2009	104/11	Algorithm Production
Landsat 5 TM	31 Jul 2009	104/12	Algorithm Production
Landsat 5 TM	4 Jul 2009	107/12	Algorithm Production
Landsat 7 ETM+	18 Jul 2008	106/11	Algorithm Production
Landsat 7 ETM+	18 Jul 2008	106/12	Algorithm Production
Landsat 5 TM	10 Jul 2007	104/11	Mapping CDOM
Landsat 5 TM	10 Jul 2007	104/12	Mapping CDOM
Landsat 7 ETM+	6 Jul 2006	105/12	Mapping CDOM
Landsat 7 ETM+	18 Jul 2005	105/12	Mapping CDOM
Landsat 7 ETM+	10 Aug 2004	104/11	Mapping CDOM
Landsat 7 ETM+	10 Aug 2004	104/12	Mapping CDOM
Landsat 7 ETM+	5 Aug 2002	104/11	Mapping CDOM
Landsat 7 ETM+	5 Aug 2002	104/12	Mapping CDOM
Landsat 7 ETM+	8 Jul 2001	105/11	Mapping CDOM
Landsat 7 ETM+	8 Jul 2001	105/12	Mapping CDOM
Landsat 7 ETM+	14 Jul 2000	104/12	Mapping CDOM

[a]"Algorithm Production" indicates that the spectral data were used to derive the empirical model (equation (2)). Scenes used for "Mapping CDOM" were not included in the model, but had equation (2) applied to spectral data from rivers and were utilized to apply the overall CDOM-DOC relationship (equation (3)) to the Landsat satellite imagery.

Polaris Project (www.thepolarisproject.org). Field sampling took place throughout July 2008 and July 2009 along the most northern ~250 km of the Kolyma River. Twenty-two river locations in 2008 and 37 locations in 2009 were sampled, including locations on the main stem of the Kolyma River and a selection of major stream and river tributaries. A range of biogeochemical parameters were sampled in both years, but here we focus on DOC and CDOM. Water samples were filtered through 0.7 μm GF/F glass fiber filters in the field and stored in acid-washed high-density polyethylene bottles without head space to minimize degassing and algal growth. DOC samples were acidified with concentrated HCl to a pH of 2 to preserve the sample until analyzed on a Shimadzu TOC-VCPH Analyzer (within one month of collection). CDOM samples were measured immediately after collection at the field station in Cherskiy as absorbance using a Thermo Scientific GENESYS 10 UV/Vis Spectrophotometer at wavelengths 200–800 nm with a 1 nm interval. Absorbance at 400 nm (a_{400}), chosen based on previous literature [e.g., *Coble*, 2007; *Kallio et al.*, 2008], was converted into an absorption coefficient ($a(\lambda)$ in units m^{-1}) as an indicator of CDOM, as in equation (1):

$$a(\lambda) = 2.303A(\lambda)/l \quad (1)$$

where $A(\lambda)$ is the absorbance and l is the cell path length in meters [*Green and Blough*, 1994].

[10] While extensive field sampling in the Kolyma River basin did not take place prior to 2008, the Pan-Arctic River Nutrients, Organic Matter, and Suspended Sediments (PARTNERS) data set provides point measurements of late summer DOC concentrations at Cherskiy from 2004 to 2006 [*McClelland et al.*, 2008]. These data were used as a first-order and independent validation of our satellite-derived CDOM and DOC estimates extrapolated over the past decade, as were additional measurements obtained by the Polaris Project in July 2010. Discharge of the Kolyma River at Kolymskoe were obtained from the Arctic-RIMS database, which were adjusted to reflect discharge of the Kolyma River at Cherskiy (located 160 km downstream of the gauging station) [e.g., *Holmes et al.*, 2011].

2.2. Remote Sensing Analysis

[11] To create an empirically based algorithm estimating CDOM using satellite imagery, we adapted methods presented by *Brezonik et al.* [2005]. Landsat TM and ETM+ imagery corresponding within two weeks of field sample collection were obtained from the U.S. Geological Survey (Table 1). The largest difference between sampling data and Landsat acquisition date was 13 d; however Kolyma River discharge varied only ~200 m^3/s (<5% of the total annual range) during this time frame. Most field samples were collected within 7 d of satellite overpass and provide a reliable basis for our comparisons [*Olmanson et al.*, 2008]. Landsat TM and ETM+ are multispectral sensors, acquiring data at 30 m resolution from spectral bands in the visible and infrared wavelengths (60–120 m resolution in thermal wavelengths) at a return interval of 16 d. In our analysis, we used bands 1–4 only: blue, green, red, and near infrared wavelengths (0.45–0.52 μm, 0.52–0.60 μm, 0.63–0.69 μm, 0.76–0.90 μm, respectively) [*Rogan and Chen*, 2004]. The remotely sensed data were atmospherically corrected and converted into reflectance values (mW cm^{-2} sr^{-1} μm^{-1}) using the Cos(t) dark-body subtraction algorithm [*Chavez*, 1996]. Rivers less than 90 m wide, comprising approximately half of the samples collected, were too narrow to be clearly apparent in the 30 m resolution Landsat imagery and were thus excluded from further analysis. Further sample sites were obscured by cloud cover and data gaps attributable to a scan line corrector error in Landsat ETM+ [*Markham et al.*, 2004]. Our final results incorporate a broad collection of observations, including seven river locations from 2008 and eleven river locations from 2009, for a total of 18 independent and geographically expansive samples (Figure 1 and Table 2). A 5 × 5 pixel window Area of Interest (AOI) was defined at each sampling location and used to extract average reflectance from visible and near infrared bands.

[12] Field-collected CDOM (a_{400}) measurements were utilized as the dependent variable in a multiple linear regression against a combination of band 1, band 2, band 3 or band 4 and multiple band ratios (e.g., band ratio 3:1). Four empirical algorithms resulted in $R^2 > 0.6$, of which the following equation (2) had the highest R^2 (0.78; p value < 0.001):

$$\ln(a_{400}) = -1.145 + 26.529(B3) + 0.603(B2:B1) \quad (2)$$

where Bx refers to reflectance in band x (1, 2 or 3) of Landsat TM or ETM+. We applied equation (2) to the Landsat TM or ETM+ imagery to produce spatial maps of CDOM and subsequently DOC concentrations along the lower 300 km of the Kolyma River using 17 scenes from 10 dates in 2000–2002 and 2004–2010 (Table 1). Landsat ETM+ encountered an error with the scan line corrector instrument in 2003, and high-quality data was not available for the Kolyma region during this year. Landsat data in 2002 and 2004 are from early August (rather than July when field sampling occurred) as cloud cover obscured all available

Table 2. DOC Concentrations, CDOM Absorption, and Available TSS Concentrations at Field Sampling Locations[a]

Sample Name	Sampling Date	DOC (mg/L)	a_{400} (m^{-1})	TSS (mg/L)	Band 1 (mW cm^{-2} sr^{-1} μm^{-1})	Band 2 (mW cm^{-2} sr^{-1} μm^{-1})	Band 3 (mW cm^{-2} sr^{-1} μm^{-1})	Band 4 (mW cm^{-2} sr^{-1} μm^{-1})
Kolyma Braid	14 Jul 2009	7.80	5.30	6.28	0.008418	0.027975	0.017994	0.008916
Kolyma 1	15 Jul 2009	3.20	2.12	11.35	0.011632	0.026856	0.009484	0.000543
Kolyma 2	17 Jul 2009	2.97	1.80	6.5	0.011606	0.026398	0.025761	0.007066
Omalon	17 Jul 2009	2.14	1.38	4.17	0.018796	0.037776	0.031633	0.008889
Kolyma 3	17 Jul 2009	3.59	1.84	9.99	0.011298	0.025487	0.025382	0.00775
Panteleikha	23 Jul 2009	6.43	3.18	5.3	0.013694	0.03498	0.026443	0.013586
Kolyma 5	24 Jul 2009	3.73	2.35	6.68	0.010162	0.027399	0.013097	0
Kolyma 6	24 Jul 2009	3.97	1.66	4.46	0.011605	0.028092	0.01407	0.000477
Kolyma 7	24 Jul 2009	4.36	2.49	4.61	0.01457	0.034281	0.021402	0
Kolyma 8	24 Jul 2009	3.68	1.84	2.54	0.014312	0.030282	0.015457	0
Kolyma 9	25 Jul 2009	3.61	1.80	12.56	0.01457	0.02984	0.014	0.002446
Kolyma 2	14 Jul 2008	7.39	4.70	–	0.025649	0.045192	0.053205	0.008752
Kolyma 3	16 Jul 2008	7.76	5.39	–	0.042166	0.052135	0.073387	0.041571
Omalon	16 Jul 2008	4.55	2.76	–	0.029946	0.043967	0.037794	0.002735
Stadukhinskaya	16 Jul 2008	7.2	4.88	–	0.041226	0.058532	0.0762	0.07357
Malinki Annui	19 Jul 2008	6.27	3.73	–	0.01128	0.028177	0.039996	0.010393
Bolshoi Annui	19 Jul 2008	9.52	6.45	–	0.001343	0.005717	0.018347	0.005196
Kolyma 5	21 Jul 2008	7.67	5.76	–	0.008418	0.027975	0.017994	0.008916

[a]Reflectance values are averages of a 5 × 5 pixel window surrounding GPS coordinates of sampling points. These CDOM and reflectance data were used in multiple linear regressions to develop equation (2).

scenes from July. However, summer DOC concentrations and composition are in general stable in arctic rivers within a given year (including the Kolyma) [*Finlay et al.*, 2006; *Neff et al.*, 2006; *Raymond et al.*, 2007], so we allowed the use of early August imagery in these cases. This is also supported by typically stable discharge of the Kolyma River during the entire time frame utilized in this study, 6 July to 10 August (Figure 2).

[13] Rivers were masked from other land cover types using a Maximum Likelihood classification (MaxLike). In addition, isolated pixels within rivers had anomalously high estimates of a_{400} (ranging from ~20–10,000 m^{-1}) likely owing to effects such as sun glint and random error. CDOM values below 20 m^{-1} were deemed reasonable, as none of our field samples exceeded this value and previous studies examining CDOM in other large arctic rivers, including the Kolyma, show that higher CDOM only occurs occasionally during spring freshet [*Retamal et al.*, 2007; *Spencer et al.*, 2008, 2009; *Stedmon et al.*, 2011]. Values exceeding 20 m^{-1} accounted for <0.5% of river pixels in each year mapped and were thus removed from the study. Last, a 3 × 3 pixel median filter was applied to smooth noise in final maps of CDOM.

3. Results

3.1. Field Measurements of DOC and CDOM

[14] DOC measured from field samples of the Kolyma River main stem and major tributaries varied between 2.14 and 9.52 mg/L (mean = 5.32 ± 2.17 (StDev) mg/L; n = 18) in July 2008 and 2009. CDOM ranged from 1.38 to 6.45 m^{-1} at 400 nm (mean = 3.3 ± 1.67 m^{-1}; n = 18). Spatially extensive field samples of both DOC and CDOM in the Kolyma main stem exhibited significant variability between 2008 and 2009. For example, in July 2008, the Kolyma main stem DOC averaged 7.61 mg/L (n = 3), while the average DOC in July 2009 was 3.64 ± 0.43 mg/L (n = 8). Streams less than 90 m wide were typified by much higher concentrations of DOC based on field samples (i.e., combined 2008 and 2009 mean = 12.8 ± 3.9 mg/L; n = 19).

[15] Past studies have shown that CDOM can be used as an inexpensive and rapid proxy for DOC in many high-latitude inland water bodies [*Baker et al.*, 2008; *Spencer et al.*, 2008, 2009; *Stedmon et al.*, 2011]. Our results support this relationship in the Kolyma River basin, as CDOM (a_{400}) correlates strongly with DOC in all available measurements from 2008 and 2009, as seen in equation (3) (R^2 = 0.86; n = 54; p value < 0.001) (Figure 3).

$$\mathrm{CDOM} = 0.4939(\mathrm{DOC}) + 0.6054 \quad (3)$$

The data used to develop this relationship include sampling points not incorporated into the empirically driven algorithm to map CDOM (equation (2)), as some sampled streams and rivers were obscured by clouds or too small to be readily apparent in Landsat satellite imagery. However, DOC and CDOM values from these smaller streams and rivers were

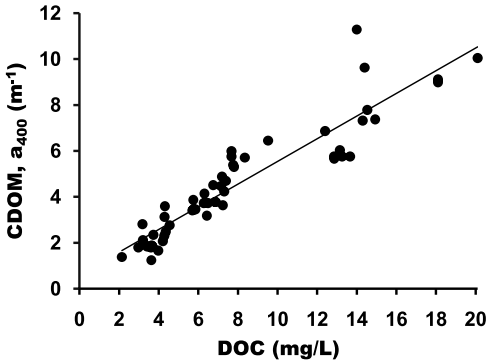

Figure 3. The relationship between dissolved organic carbon (DOC) and CDOM in the Kolyma River, using 54 field observations from July 2008 and 2009. (CDOM = 0.494 (DOC) + 0.605; R^2 = 0.86; p value < 0.01; equation (3)).

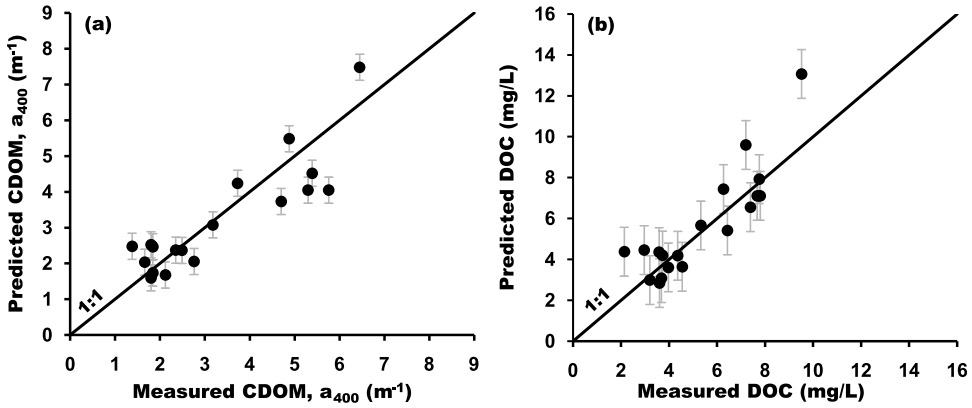

Figure 4. (a) Predicted CDOM absorption at 400 nm (m^{-1}) (based on Landsat TM and ETM+ reflectance data) versus measured CDOM absorption at 400 nm (m^{-1}) (based on field observations) ($CDOM_{predicted}$ = 0.816*($CDOM_{measured}$) + 0.525; R^2 = 0.77; p value < 0.00001). (b) Satellite-predicted DOC in mg/L (based on both equations (2) and (3)) versus measured DOC (based on field observations) ($DOC_{predicted}$ = 1.08*($DOC_{measured}$) – 0.087; R^2 = 0.76; p value < 0.00001).

included in equation (3) in order to constrain the higher concentrations that emerged when applying this equation to the remotely sensed data then available for only the large rivers.

3.2. Empirically Derived Algorithms for Landsat Satellite Data

[16] Multiple regression analyses between ln(a_{400}) and a combination of band 3 and the band 2:band 1 ratio resulted in equation (2), (R^2 = 0.78). Figure 4a illustrates the relationship between field-based measurements of a_{400} and satellite-based predicted a_{400} obtained using equation (2), with standard error bars included. All sampling locations fit the regression well: All predicted CDOM values are within approximately 1 m^{-1} of measured CDOM, with the exception of one measurement from a braid in the Kolyma in 2009. Estimated CDOM values were then converted into DOC concentrations using equation (3), and plotted to evaluate the ability of remote sensing techniques to estimate DOC (with CDOM as the intermediary) (Figure 4b). Error propagation to the final satellite-based DOC concentrations was calculated using the following equation (4) [*Taylor*, 1997]:

$$\frac{\delta q}{|q|} = \sqrt{\left(\frac{\delta x}{x}\right)^2 + \left(\frac{\delta y}{y}\right)^2} \quad (4)$$

Where δ indicates uncertainty, q is satellite-derived DOC, x is satellite-derived CDOM, and y is the estimated DOC based on the established field-derived DOC-CDOM relationship. The standard error in the satellite-derived CDOM estimates is ±0.76 m^{-1}, the standard error in DOC estimates (from our field-based DOC-CDOM relationship) is ±0.92 mg/L, whereas the propagated error in satellite-derived DOC estimates (based on equation (4)) averages ±1.68 mg/L. Although error propagation leads to slightly higher uncertainties in satellite-derived estimates of DOC than CDOM, the correlation between measured and predicted DOC is still quite high (R^2 = 0.75; p value <0.0001). Having established these empirical relationships between remotely sensed data and field measurements of CDOM and DOC, we applied equations (2) and (3) to our masked river and main stem regions in the Landsat scenes for ten years over the past decade (2000–2002 and 2004–2010). These maps enhance our ability to observe spatial and interannual variability in CDOM and DOC across the entire region (Figure 5).

3.3. Spatial Patterns

[17] Certain spatial patterns are common across all maps of CDOM and DOC for all years in this study. Profiles of CDOM and DOC concentrations extracted from a 300 km transect down the center of the river main stem (shown with a 5 km running mean) provide an additional way to visualize patterns and variability within the Kolyma River (Figure 6). In most years, there is a general downstream increase in concentrations in the Kolyma main stem (Figures 5 and 6). In particular, most years are characterized by a sharp increase in CDOM approximately 190 km along a profile of the main stem, followed by either consistently higher concentrations or a gradual increase toward the Arctic Ocean (Figure 6). This feature corresponds roughly with the location where the Kolyma River branches into two major main stem sections north of Cherskiy as it approaches the Arctic Ocean.

[18] Beyond the point where the Kolyma diverges into its major east-west branches north of Cherskiy, both branches generally continue to increase in DOC concentrations relative to upstream values. However, the western branch consistently displays markedly higher CDOM and DOC concentrations, particularly in 2001 and 2002 (Figure 5). For instance, the eastern branch in 2001 is characterized by DOC concentrations of ~8.5 mg/L 30 km downstream of Cherskiy, while the western branch is typified by DOC concentrations of ~12 mg/L at similar latitudes. While this is the most extreme difference observed, all years except 2008 and 2009 have noticeable differences between the eastern and western branches of the river.

[19] In addition to these variations within the Kolyma itself, the three major tributaries within our study area

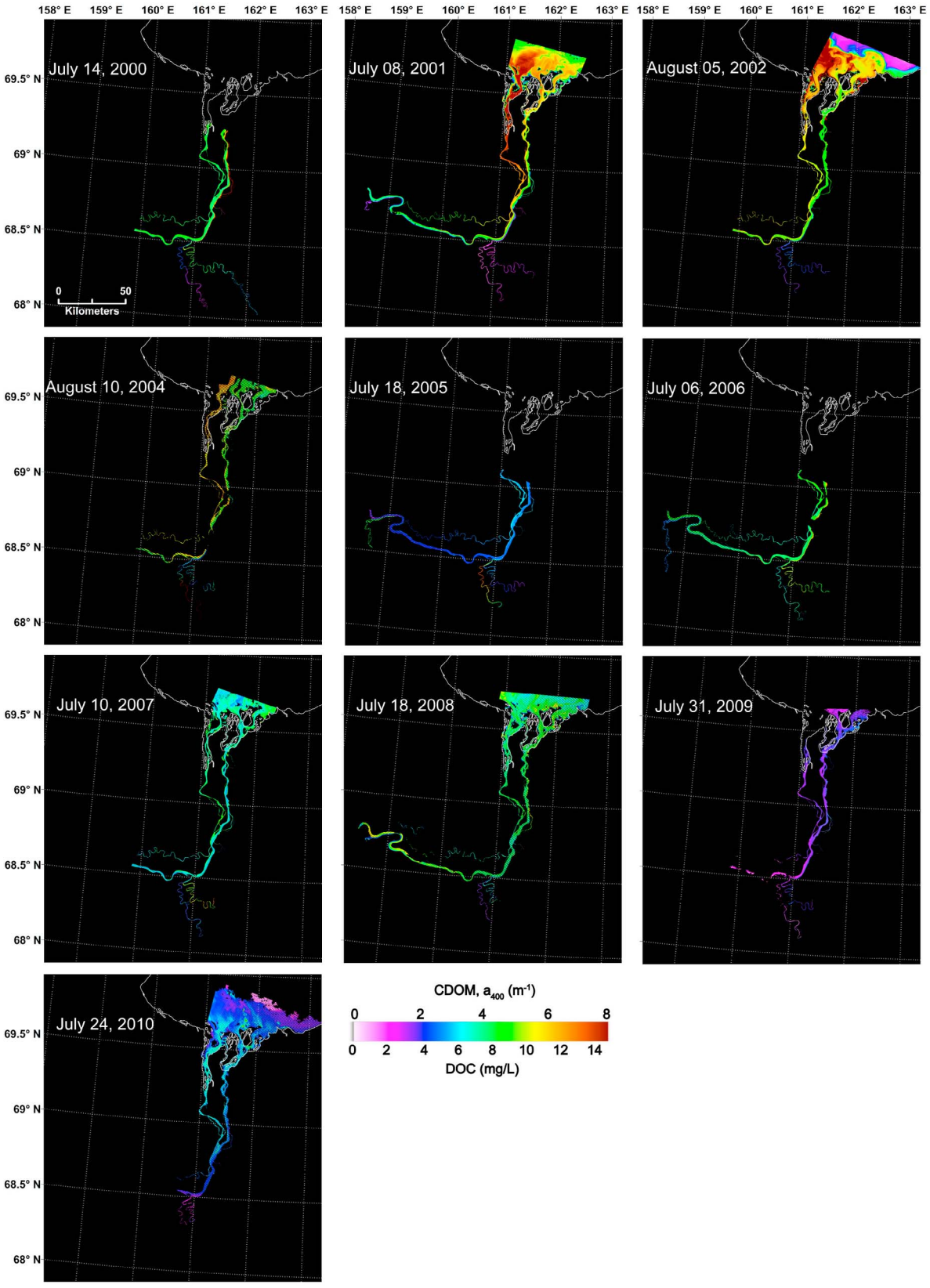

Figure 5. Mapped CDOM and DOC during summer of 2000–2002 and 2004–2010. The best produced multiple linear regression equation (utilizing band 3 and the bands 2:1 ratio; equation (2)) was applied to the atmospherically corrected Landsat satellite data to produce estimates of CDOM and DOC concentrations for the Kolyma River and its major tributaries.

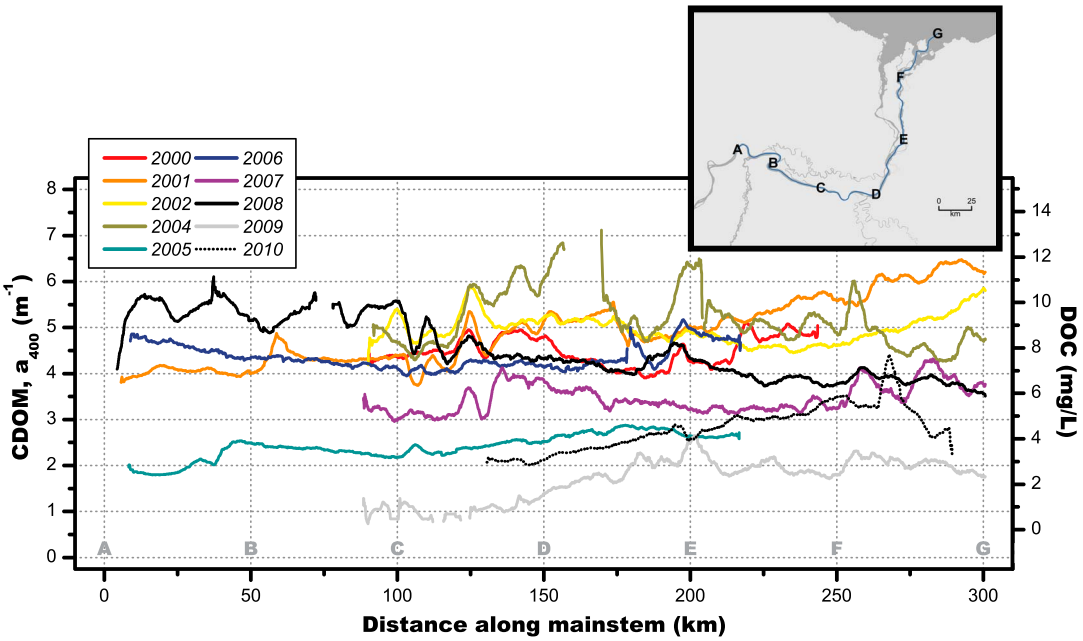

Figure 6. Profiles of CDOM and DOC extracted from satellite-based mapped concentrations.

(Omalon River, Bolshoi Annui, and Malinki Annui; Figure 1) often differ starkly in CDOM and DOC concentrations from the main stem (Figure 5). Most maps show lower CDOM and DOC concentrations in these rivers than in the Kolyma. For instance, the Kolyma main stem in 2001 is characterized by DOC of ~8 mg/L, while Omalon DOC concentrations are ~3 mg/L and the Bolshoi Annui and Malinki Annui tend to have concentrations of ~2–3 mg/L. However, there are exceptions to this general rule, as found in 2005. In this year, DOC in both the Kolyma River and Malinki Annui is ~5 mg/L, but concentrations in the Omalon are >8 mg/L and in the Bolshoi Annui are >12 mg/L. Additionally, the Bolshoi Annui exceeds Kolyma River concentrations by 4 mg/L in August 2004 and the Malinki Annui surpasses the Kolyma main stem by ~2–3 mg/L in 2007 and ~1–2 mg/L in 2009.

[20] These differences in DOM concentrations between the Kolyma and its major tributaries often result in striking mixing zones that consistently extend far downstream (Figure 5). Mixing zones caused by the confluence of the Bolshoi Annui and Malinki Annui into the Kolyma main stem can be seen throughout all our maps. In some maps, such as 2001, 2002, and 2008, water contributed by the tributaries can be distinctly identified as far as Cherskiy, 40 km downstream of where the tributaries initially drain into the Kolyma. Similar mixing zones are also associated with the Omalon River and other smaller tributaries throughout the region.

3.4. Interannual Variability

[21] The highest overall CDOM and DOC concentrations across the region were estimated in 2001 and 2004, while the lowest overall concentrations were found in 2005, 2009, and 2010 (Figures 4 and 5). Most years are characterized by CDOM values clustered between of 4–5.5 m^{-1}. However, CDOM estimates in 2005, 2009 and 2010 are distinctly lower than this. To better quantify the differences between years, we extracted the average CDOM in a 4 × 4 pixel AOI located at a representative point of the Kolyma River main stem near Cherskiy. On the basis of this point, average summer (July-August) satellite-based CDOM is 3.69 ± 0.98 m^{-1} (n = 10), which corresponds to an average DOC of 6.49 ± 1.79 mg/L (n = 10). Overall, main stem concentrations along a 300 km transect range from ~2–12 mg/L (Figure 6). Even higher concentrations of 14 mg/L or more are estimated in the western branch of the Kolyma. Tributaries of the Kolyma vary to a similar degree, with

Table 3. Comparison of Measured DOC and Predicted DOC From Satellite-Based Modeled Results[a]

Year	Predicted CDOM (a_{400})	Predicted DOC (mg/L)	Measured DOC (mg/L)	TSS (mg/L)	Image Date	Sampling Date
2004	3.99	7.00	3.92	30.3	10 Aug 2004	10 Aug 2004
2005	3.09	5.44	4.41	12	18 Jul 2005	19 Jul 2005
2006	4.56	8.00	8.66	11.1	6 Jul 2006	24 Jul 2006
2010	2.44	4.32	4.04	-	24 Jul 2010	27 Jul 2010

[a]Measurements from 2004 to 2006 are from the PARTNERS data set, and 2010 data are from the Polaris Project. Erroneous satellite-based estimations of CDOM and DOC in 2004 may be attributable to relatively high total suspended solids concentrations.

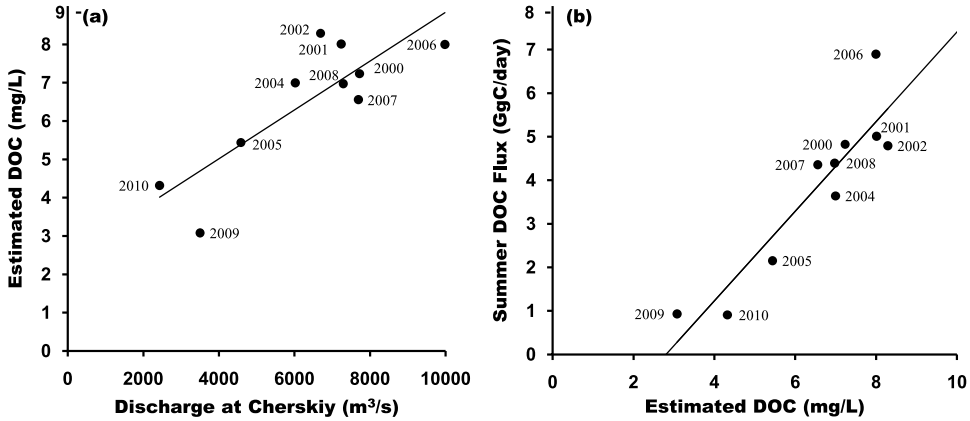

Figure 7. (a) There is a general positive linear relationship between discharge and satellite-derived DOC concentrations at Cherskiy during July and August 2000–2010 (DOC = 0.0006375 * (Q) + 2.465; R^2 = 0.70; p value < 0.01). (b) Correlation between satellite-derived DOC concentrations and DOC flux calculated using discharge at Cherskiy and satellite-derived DOC estimates during July and August 2000–2010 (flux = 1.029*(DOC) + −2.890; R^2 = 0.84; p value < 0.001).

DOC concentrations ranging ~2–14 mg/L, although these rivers seem to vary independently of concentrations within the main stem.

[22] We use PARTNERS data from 2004 to 2006 [*McClelland et al.*, 2008] and a sample from the 2010 field season of the Polaris Project, all collected at points in the Kolyma near Cherskiy, to independently validate our satellite-based estimates of CDOM and DOC (Table 3). Satellite-derived and field measured DOC match well in 2005, 2006 and 2010. The poorest agreement exists in 2004, when satellite-derived DOC exceeds field measurements by over 3 mg/L. This year also exhibits total suspended solids (TSS) concentrations several times higher than other PARTNERS samples from July and August, or samples collected in 2009 (Tables 2 and 3).

4. Discussion

[23] Most previous studies addressing Kolyma River DOC concentrations consider only points along the main stem of the river near Cherskiy, or may include a small number of nearby tributaries and lowland streams [*Finlay et al.*, 2006; *Neff et al.*, 2006; *Holmes et al.*, 2011]. However, here we show there are significant spatial patterns and heterogeneity within the lower Kolyma river watershed, which may be used to guide the execution and direction of future research. For instance, our maps of CDOM and DOC highlight the importance of carefully selecting sampling locations when characterizing the biogeochemistry of the Kolyma main stem. Major mixing zones can extend up to 40 km downstream and hundreds of meters across the main stem where a tributary meets the Kolyma River, such that nearshore point-based field collections of waters may not necessarily be representative of the river as a whole.

[24] Additional spatial patterns occur consistently throughout our maps of DOC, which have not been observed previously using field-based point measurements. The Kolyma main stem is characterized by a general downstream increase in DOC concentrations (Figures 5 and 6). This pattern was also observed in extensive field samples along the Kolyma in 2009, and is thus unlikely to be an artifact of the digital image processing. It is possible that DOC in colder, more northerly watersheds may not be consumed through microbial activity within streams before tributaries join the Kolyma. Alternatively, refractory DOC may accumulate in the main stem as labile fractions are consumed along the river flowpath. The general increase in DOC approaching the Arctic Ocean also varies between the two main branches of the Kolyma north of Cherskiy. In most years (particularly 2001, 2002 and 2010) the western branch is characterized by markedly higher CDOM and DOC than the eastern branch. Although no previous studies sample the western branch of the Kolyma, visual inspection of satellite images reveals that many small streams draining organic matter rich lowlands west of the Kolyma join this branch, perhaps explaining why DOC concentrations are elevated here. Our satellite-based maps of CDOM and DOC thus show significant amounts of spatial heterogeneity that may be linked to differences in subwatershed climate, land cover, and organic matter content.

[25] Typically, DOC concentrations in arctic rivers, including the Kolyma, are markedly higher during the spring freshet, and lower and more stable through time from July–October [*Raymond et al.*, 2007; *Holmes et al.*, 2011]. However, our results also show significant interannual variability in summer concentrations. In fact, the range in DOC concentrations across summers for different years (based on our satellite observations over the past decade) is similar to the overall seasonal variability in DOC concentrations throughout an entire given year. For instance, maximum DOC in 2004 from the PARTNERS data set was 10.27 mg/L (sampled on 11 June 2004, one week after peak discharge), while the minimum was 3.91 mg/L (sampled on 23 September 2004), for a total range of 6.36 mg/L. In comparison, our estimates of summer DOC at Cherskiy extend from 3.08 mg/L in 2009 to 8.29 mg/L in 2002 (Figure 6), for a total range of 5.21 mg/L. As with seasonal variations in DOC, discharge is likely a major factor in the interannual variability in DOC concentrations during July and August (Figure 7a). Figure 7b shows that this has important impli-

cations for summer flux estimates, plotted as a function of discharge and satellite-derived DOC. On the basis of these relationships, we see no dilution effect that would cause fluxes in high flow conditions to be offset by low concentrations of DOC during July and August. These results are corroborated by previous research on the Kolyma and other large arctic rivers, where it is known that discharge is the primary driver of seasonal variation in DOC [*Finlay et al.*, 2006; *Holmes et al.*, 2011].

[26] While remotely sensed data have proved effective as a proxy for CDOM and DOC concentrations for most years in this study (when compared to field observations), there is a difference of 3.08 mg/L between satellite-derived and measured DOC in 2004 (Table 3). Visual inspection of 2004 Landsat ETM+ true color composites reveals that exceptionally high CDOM values correspond with rivers that appear a turbid brown color, most likely owing to high TSS concentrations that were also observed by PARTNERS field measurements (Table 3). This interference between TSS and satellite reflectance data may also explain why the 2004 profile in Figure 6 varies more erratically than other years. While it is possible that TSS could be influencing our mapped CDOM in years without reference field data (e.g., 2000–2002), Landsat composites from all other years show no evidence of the turbid brown river water that appears in the 2004 composite. On the basis of our experience in this study, when TSS concentrations exceed approximately 15 mg/L in summer months, the resulting optical characteristics may obscure the signal of CDOM in satellite data by increasing reflectance. Remote sensing has a long history of estimating suspended sediment concentration (SSC; the inorganic portion of TSS) from Landsat data [e.g., *Ritchie et al.*, 2003; *Pavelsky and Smith*, 2009]. Unfortunately, TSS or SSC were not consistently measured during 2008 and 2009 field campaigns (Table 2) and there are no data sets available to characterize temporal variability at daily time scales. However, despite the potential optical interference of suspended sediments, TSS concentrations are typically low in our study region and generally unlikely to greatly influence estimates of DOC or CDOM during this July–August timeframe.

[27] These new observations of variability are important to consider when calculating flux estimates of DOC to the Arctic Ocean. Although the majority of discharge and DOC export occurs during spring months, July–October accounts for nearly half of annual discharge and over one third of annual DOC export [*Holmes et al.*, 2011], making summer variability an important factor in annual flux estimates. Previous studies using discharge models to estimate total flux [e.g., *Manizza et al.*, 2009; *Holmes et al.*, 2011] do not account for our new observations of spatial heterogeneity and increases in DOC concentrations downstream of their sampling location at Cherskiy (e.g., the western branch of the Kolyma main stem). In addition, multiple recent studies that model DOC export are based upon field data for one or more years from 2003 to 2006, collected at a single location [e.g., *Finlay et al.*, 2006; *Neff et al.*, 2006; *Manizza et al.*, 2009; *Holmes et al.*, 2011]. Summer DOC concentrations (as well as river runoff) in three of these years are lower than average values for the last decade observed from our satellite-based maps, suggesting that these currently available flux calculations may be underestimates. We can further speculate that years with relatively high DOC concentrations and runoff during summer may also have higher DOC during spring freshet (when the majority of DOC flux occurs [*Holmes et al.*, 2011]), potentially resulting in even greater underestimates in total annual flux of DOC. Our broad satellite-based observations of DOC across the Kolyma River region allow for a new opportunity to spatially and temporally extrapolate point field observations to assess the validity of current export estimates. When both the spatial and interannual variability in DOC concentrations are taken into account, the total flux of DOC likely varies dramatically from year to year and current approximations may be underestimating overall carbon export to the Arctic Ocean.

5. Implications and Conclusions

[28] Arctic hydrology is undergoing profound changes as climate warming causes a regional acceleration of the hydrological cycle [*ACIA*, 2005; *White et al.*, 2007]. In particular, shifting terrestrial ecosystems, degrading permafrost, and increasing river discharge will have as yet uncertain impacts on DOC concentrations and fluxes [*Wickland et al.*, 2007; *Frey and McClelland*, 2009]. Many studies illustrate a positive correlation between DOC and river discharge [e.g., *McClelland et al.*, 2007; *Raymond et al.*, 2007] and DOC flux to the Arctic Ocean is often calculated based upon these observed relationships [*Raymond et al.*, 2007; *Manizza et al.*, 2009; *Holmes et al.*, 2011]. However, there is no guarantee that the current, observed relationships between discharge and DOC concentrations are constant through time and will be applicable in future conditions. The potential for permafrost degradation to influence DOC export within the Kolyma basin is of particular importance, particularly to summer fluxes. Vast reserves of old organic matter, which laboratory incubations show are potentially reactive once released, are stored in the basin's permafrost soils [*Zimov et al.*, 2006a, 2006b]. Although the exact age of summer DOC in the Kolyma River is unknown, low abundances of lignin biomarkers and low specific UV absorbance (SUVA) measurements suggest summer DOC is largely derived from permafrost and soil organic matter [*Neff et al.*, 2006]. Indeed, increased active layer depths have been observed across the Siberian Arctic by a number of studies, indicating that a change in carbon storage may already be occurring in some regions. Release of this old carbon into hydrologic flowpaths may not be dependent upon discharge, and thus difficult to model based solely on discharge-DOC relationships. Furthermore, river discharge across the Siberian Arctic has increased over the last half century [*Peterson et al.*, 2002], likely a result of increased precipitation [*Pavelsky and Smith*, 2006]. The effects of these changing hydrological patterns on the relationship between discharge and DOC have yet to be fully constrained. Remote sensing thus offers an additional method to supplement field observations, by directly measuring the actual properties of the river, rather than relying upon modeling that may not account for these multiple, confounding factors.

[29] Intrinsic variability and longer-term trends in carbon cycling of the Kolyma River basin are both important to understand in light of the vast reserves of carbon locked away in Pleistocene-aged permafrost that could potentially degrade with climate warming in the coming century [*Zimov*

et al., 2006; *Schuur et al.*, 2008]. Using remote sensing techniques, we show here that summer (July–August) CDOM concentrations, as a proxy for DOC, exhibit distinct spatial patterns and significant interannual variability across the northern Kolyma River basin over the last decade. These previously unobserved variations in DOC have important implications for estimates of DOC flux to the Arctic Ocean. For instance, the western branch of the Kolyma is characterized by elevated DOC concentrations relative to upstream locations, suggesting that current calculations of DOC flux from the Kolyma River to the Arctic Ocean may be underestimates. The interannual variability in DOC found in this study over the past decade is also higher than observed with previously available limited field measurements from 2003 to 2006. Furthermore, these satellite-derived estimates will thus be useful for recalibrating DOC export-discharge models if relationships between DOC and river discharge change owing to shifting hydrological regimes, thawing permafrost, or increasing terrestrial productivity. Large-scale and systematic monitoring of organic carbon concentrations in major arctic river systems using methods such as satellite remote sensing is therefore critically important to our understanding of the arctic carbon cycle, particularly in light of the region's rapid climate change and potentially significant impacts on the riverine delivery of organic matter to the Arctic Ocean.

[30] **Acknowledgments.** This work was supported by the National Science Foundation as part of the Polaris Project (http://www.thepolarisproject.org/) (NSF-0732586 and NSF-0732944) and Arctic Great Rivers Observatory (Arctic-GRO) (NSF-0732522). We thank Alexander Shiklomanov for providing discharge data for the Kolyma River and Ekaterina Bulygina, Andy Bunn, Sudeep Chandra, Sergei Davydov, Anya Davydova, Blaize Denfeld, John Schade, Bill Sobczak, Valentin Spektor, Katey Walter-Anthony, Kate Willis, Nikita Zimov, and Sergei Zimov for assistance with sample collection and/or project coordination. We would additionally like to thank the two anonymous reviewers for their helpful comments and suggestions.

References

Arctic Climate Impact Assessment (ACIA) (2005), *Impacts of a Warming Arctic: Arctic Climate Impact Assessment*, Cambridge Univ. Press, Cambridge, U. K.

Anderson, L. G., S. Jutterstrom, S. Hjalmarsson, I. Wahlstrom, and I. P. Semilitov (2009), Out-gassing of CO_2 from Siberian Shelf seas by terrestrial matter decomposition, *Geophys. Res. Lett.*, *36*, L20601, doi:10.1029/2009GL040046.

Baker, A., L. Bolton, M. Newson, and R. G. M. Spencer (2008), Spectrophotometric properties of surface water dissolved organic matter in an afforested upland peat catchment, *Hydrol. Process.*, *22*(13), 2325–2336, doi:10.1002/hyp.6827.

Battin, T. J., S. Luyssaert, L. A. Kaplan, A. K. Aufdenkampe, A. Richter, and L. J. Tranvik (2009), The boundless carbon cycle, *Nat. Geosci.*, *2*, 598–600, doi:10.1038/ngeo618.

Brezonik, P., K. D. Menken, and M. Bauer (2005), Landsat-based remote sensing of lake water quality characteristics, including chlorophyll and colored dissolved organic matter (CDOM), *Lake Reservior Manage.*, *21*(4), 373–382, doi:10.1080/07438140509354442.

Chavez, P. S. J. (1996), Image-based atmospheric corrections–revisited and improved, *Am. Soc. Photogramm. Remote Sens.*, *62*(9), 1025–1036.

Coble, P. (2007), Marine optical biogeochemistry: The chemistry of ocean color, *Chem. Rev.*, *107*(2), 402–418, doi:10.1021/cr050350+.

Cole, J. J., et al. (2007), Plumbing the global carbon cycle: Integrating inland waters into the terrestrial carbon budget, *Ecosystems*, *10*(1), 172–185, doi:10.1007/s10021-006-9013-8.

Cooper, L. W., R. Benner, J. W. McClelland, B. J. Peterson, R. M. Holmes, P. A. Raymond, D. A. Hansell, J. M. Grebmeier, and L. A. Codispoti (2005), Linkages among runoff, dissolved organic carbon, and the stable oxygen isotope composition of seawater and other mass indicators in the Arctic Ocean, *J. Geophys. Res.*, *110*, G02013, doi:10.1029/2005JG000031.

Dittmar, T., and G. Kattner (2003), The biogeochemistry of the river and shelf ecosystem of the Arctic Ocean: A review, *Mar. Chem.*, *83*(3–4), 102–120.

Finlay, J., J. Neff, S. Zimov, A. Davydova, and S. Davydov (2006), Snowmelt dominance of dissolved organic carbon in high-latitude watersheds: Implications for characterization and flux of river DOC, *Geophys. Res. Lett.*, *33*, L10401, doi:10.1029/2006GL025754.

Frey, K. E., and J. W. McClelland (2009), Impacts of permafrost degradation on arctic river biogeochemistry, *Hydrol. Process.*, *23*(1), 169–182, doi:10.1002/hyp.7196.

Frey, K. E., and L. C. Smith (2005), Amplified carbon release from vast West Siberian peatlands by 2100, *Geophys. Res. Lett.*, *32*, L09401, doi:10.1029/2004GL022025.

Frey, K. E., J. W. McClelland, R. M. Holmes, and L. C. Smith (2007), Impacts of climate warming and permafrost thaw on the riverine transport of nitrogen and phosphorous to the Kara Sea, *J. Geophys. Res.*, *112*, G04S58, doi:10.1029/2006JG000369.

Garneau, M. E., S. Roy, C. Lovejoy, Y. Gratton, and W. F. Vincent (2008), Seasonal dynamics of bacterial biomass and production in a coastal arctic ecosystem: Franlin Bay, western Canada, *J. Geophys. Res.*, *113*, C07S91, doi:10.1029/2007JC004281.

Green, S. A., and N. V. Blough (1994), Optical absorption and fluorescence properties of chromophoric dissolved organic matter in natural waters, *Limnol. Oceanogr.*, *39*(8), 1903–1916, doi:10.4319/lo.1994.39.8.1903.

Holmes, R. M., J. W. McClelland, P. A. Raymond, B. B. Frazer, B. J. Peterson, and M. Stieglitz (2008), Lability of DOC transported by Alaskan rivers to the Arctic Ocean, *Geophys. Res. Lett.*, *35*, L03402, doi:10.1029/2007GL032837.

Holmes, R. M., K. E. Frey, and S. Zimov (2009), A field course in the Siberian Arctic: 30 days, 20 people, 3 continents, 1 barge, *Eos Trans. AGU*, *90*(26), doi:10.1029/2009EO260003.

Holmes, R. M., et al. (2011), Seasonal and annual fluxes of nutrients and organic matter from large rivers to the Arctic Ocean and surrounding seas, *Estuaries Coasts*, doi:10.1007/s12237-011-9386-6.

Kallio, K., J. Attila, P. Harma, S. Koponen, J. Pulliainen, U. M. Hyytiainen, and T. Pyhalahti (2008), Landsat ETM+ images in the estimation of seasonal lake water quality in Boreal river basins, *Environ. Manage.*, *42*, 511–522, doi:10.1007/s00267-008-9146-y.

Kutser, T., D. C. Pierson, K. Kallio, A. Reinart, and S. Sobek (2005a), Mapping lake CDOM by satellite remote sensing, *Remote Sens. Environ.*, *94*, 535–540, doi:10.1016/j.rse.2004.11.009.

Kutser, T., D. C. Pierson, L. Tanvik, A. Reinart, S. Sobek, and K. Kallio (2005b), Using satellite remote sensing to estimate the colored dissolved organic matter absorption coefficient in lakes, *Ecosystems*, *8*, 709–720 doi:10.1007/s10021-003-0148-6.

Manizza, M., et al. (2009), Modeling transport and fate of riverine dissolved organic carbon in the Arctic Ocean, *Global Biogeochem. Cycles*, *23*, GB4006, doi:10.1029/2008GB003396.

Markham, B. L., J. C. Storey, D. L. Williams, and J. R. Irons (2004), Landsat sensor performance: History and current status, *IEEE Trans. Geosci. Remote Sens.*, *42*(12), 2691–2694, doi:10.1109/TGRS.2004.840720.

McClelland, J. W., S. J. Dery, B. J. Peterson, R. M. Holmes, and E. F. Wood (2006), A pan-Arctic evaluation of changes in river discharge during the latter half of the 20th century, *Geophys. Res. Lett.*, *33*, L06715, doi:10.1029/2006GL025753.

McClelland, J. W., M. Stieglitz, F. Pan, R. M. Holmes, and B. J. Peterson (2007), Recent changes in nitrate and dissolved organic carbon export from the upper Kuparuk River, North Slope, Alaska, *J. Geophys. Res.*, *112*, G04S60, doi:10.1029/2006JG000371.

McClelland, J. W., et al. (2008), Development of a pan-Arctic database for river chemistry, *Eos Trans. AGU*, *89*(24), 217–218, doi:10.1029/2008EO240001.

Moore, T. R. (2003), Dissolved organic carbon in a northern boreal landscape, *Global Biogeochem. Cycles*, *17*(4), 1109, doi:10.1029/2003GB002050.

Neff, J. C., J. C. Finlay, S. A. Zimov, S. P. Davydov, J. J. Carrasco, E. A. Schuur, and A. I. Davydova (2006), Seasonal changes in the age and structure of dissolved organic carbon in Siberian rivers and streams, *Geophys. Res. Lett.*, *33*, L23401, doi:10.1029/2006GL028222.

Olmanson, L. G., M. E. Bauer, and P. L. Brezonik (2008), A 20-year Landsat water clarity census of Minnesota's 10,000 lakes, *Remote Sens. Environ.*, *112*, 4086–4097, doi:10.1016/j.rse.2007.12.013.

Opsahl, S., R. Benner, and R. M. W. Amon (1999), Major flux of terrigenous dissolved organic matter through the Arctic Ocean, *Limnol. Oceanogr.*, *44*(8), 2017–2023, doi:10.4319/lo.1999.44.8.2017.

Pavelsky, T. M., and L. C. Smith (2006), Intercomparison of four global precipitation data sets and their correlation with increased Eurasian river

discharge to the Arctic Ocean, *J. Geophys. Res.*, *111*, D21112, doi:10.1029/2006JD007230.

Pavelsky, T. M., and L. C. Smith (2009), Remote sensing of suspended sediment concentration, flow velocity, and lake recharge in the Peace-Athabasca Delta, Canada, *Water Resour. Res.*, *45*, W11417, doi:10.1029/2008WR007424.

Peterson, B. J., R. M. Holmes, J. W. McClelland, C. J. Vorosmarty, R. B. Lammers, A. I. Shiklomanov, I. A. Shiklomanov, and S. Rahmstorf (2002), Increasing river discharge to the Arctic Ocean, *Science*, *298*, 2171–2173, doi:10.1126/science.1077445.

Raymond, P. A., J. W. McClelland, R. M. Holmes, A. V. Zhulidov, K. Mull, B. J. Peterson, R. G. Striegl, G. R. Aiken, and T. Gutorvaya (2007), Flux and age of dissolved organic carbon exported to the Arctic Ocean: A carbon isotopic study of the five largest arctic rivers, *Global Biogeochem. Cycles*, *21*, GB4011, doi:10.1029/2007GB002934.

Retamal, L., S. Bonilla, and W. F. Vincent (2007), Optical gradients and phytoplankton production in the Mackenzie River and the coastal Beaufort Sea, *Polar Biol.*, *31*(3), 363–379, doi:10.1007/s00300-007-0365-0. [Printed 2008.]

Ritchie, J. C., P. V. Zimba, and J. H. Everitt (2003), Remote sensing techniques to assess water quality, *Photogramm. Eng. Remote Sens.*, *63*(6), 695–704.

Rogan, J., and D. M. Chen (2004), Remote sensing technology for mapping and monitoring land-cover and land-use change, *Prog. Plann.*, *61*(4), 301–325, doi:10.1016/S0305-9006(03)00066-7.

Schuur, E. A. G., et al. (2008), Vulnerability of permafrost carbon to climate change: Implications for the global carbon cycle, *BioScience*, *58*(8), 701–714, doi:10.1641/B580807.

Smith, L. C., Y. Sheng, G. M. MacDonald, and L. D. Hinzman (2005), Disappearing arctic lakes, *Science*, *308*, 1429, doi:10.1126/science.1108142.

Spencer, R. G. M., G. R. Aiken, K. P. Wickland, R. G. Striegl, and P. J. Hernes (2008), Seasonal and spatial variability in dissolved organic matter quantity and composition from the Yukon River basin, Alaska, *Global Biogeochem. Cycles*, *22*, GB4002, doi:10.1029/2008GB003231.

Spencer, R. G. M., A. R. Aiken, K. D. Butler, M. M. Dornblaser, R. G. Striegl, and P. J. Hernes (2009), Utilizing chromophoric dissolved organic matter measurements to derive export and reactivity of dissolved organic carbon exported to the Arctic Ocean: A case study of the Yukon River, Alaska, *Geophys. Res. Lett.*, *36*, L06401, doi:10.1029/2008GL036831.

Stedmon, C. A., R. M. W. Amon, A. J. Rinehart, and S. A. Walker (2011), The supply and characteristics of colored dissolved organic matter (CDOM) in the Arctic Ocean: Pan Arctic trends and differences, *Mar. Chem.*, *124*, 108–118, doi:10.1016/j.marchem.2010.12.007.

Striegl, R. G., A. R. Aiken, M. M. Dornblaser, P. A. Raymond, and K. P. Wickland (2005), A decrease in discharge-normalized DOC export by the Yukon River during summer through autumn, *Geophys. Res. Lett.*, *32*, L21413, doi:10.1029/2005GL024413.

Tarnocai, C., J. G. Canadell, E. A. G. Schuur, P. Kuhry, G. Mazhitova, and S. Zimov (2009), Soil organic carbon pools in the northern circumpolar permafrost region, *Global Biogeochem. Cycles*, *23*, GB2023, doi:10.1029/2008GB003327.

Taylor, J. R. (1997), *An Introduction to Error Analysis: The Study of Uncertainties in Physical Measurements*, 2nd ed., Univ. Sci., Sausalito, Calif.

Twardowski, M. S., M. R. Lewis, A. H. Barnard, and J. R. V. Zaneveld (2005), In-water instrumentation and platforms for ocean color remote sensing applications, in *Remote Sensing of Coastal Aquatic Environments*, edited by R. L. Miller et al., pp. 69–100, Springer, Dordrecht, Netherlands, doi:10.1007/978-1-4020-3100-7_4.

Wang, M., and J. E. Overland (2009), A sea ice free summer Arctic within 30 years?, *Geophys. Res. Lett.*, *36*, L07502, doi:10.1029/2009GL037820.

White, D., et al. (2007), The arctic freshwater system: Changes and impacts, *J. Geophys. Res.*, *112*, G04S54, doi:10.1029/2006JG000353.

Wickland, K. P., J. C. Neff, and G. R. Aiken (2007), Dissolved organic carbon in Alaskan boreal forest: Sources, chemical characteristics, and biodegradability, *Ecosystems*, *10*(8), 1323–1340, doi:10.1007/s10021-007-9101-4.

Zimov, S. A., E. A. G. Schuur, and F. S. Chapin (2006a), Permafrost and the global carbon budget, *Science*, *312*, 1612–1613, doi:10.1126/science.1128908.

Zimov, S. A., S. P. Davydov, G. M. Zimova, A. I Davydova, E. A. G. Schuur, K. Dutta, and F. S. Chapin (2006b), Permafrost carbon: Stock and decomposability of a globally significant carbon pool, *Geophys. Res. Lett.*, *33*, L20502, doi:10.1029/2006GL027484.

K. E. Frey and J. Rogan, Graduate School of Geography, Clark University, Worcester, MA 01610, USA.

C. G. Griffin, Marine Science Institute, University of Texas at Austin, Port Aransas, TX 78373, USA. (claire.griffin@mail.utexas.edu)

R. M. Holmes, Woods Hole Research Center, Falmouth, MA 02540, USA.